

# Strong-field two-photon absorption in atomic cesium: an analytical control approach

Sangkyung Lee, Jongseok Lim, and Jaewook Ahn

*Department of Physics, KAIST, Daejeon 305-701, South Korea*

[jwahn@kaist.ac.kr](mailto:jwahn@kaist.ac.kr)

**Abstract:** We have considered an analytical control of two-photon absorption process of atoms in the strong-field interaction regime. The experiment was performed on gaseous cesium atoms strongly interacting with a shaped laser-pulse from a femtosecond laser amplifier and a programmable pulse-shaper. When this shaped laser-pulse transfers the atomic population from the  $6s$  ground state to the  $8s$  excited state, we have found that both positively- and negatively-chirped laser pulses, compared with a Gaussian pulse, enhance this excitation in the strong-field regime of laser-atom interaction. This unusual phenomena is explained because the temporal shape of the laser intensity compensates the effect of dynamic Stark shift for the two-photon resonant condition to be optimally maintained. We provide analytic calculations using the strong-field phase matching, which show good agreement with the experiment.

© 2009 Optical Society of America

**OCIS codes:** (190.7110) Ultrafast nonlinear optics; (190.4180) Multiphoton processes; (320.5540) Pulse shaping.

---

## References and links

1. K. Bergmann, H. Theuer, and B. W. Shore, "Coherent population transfer among quantum states of atoms and molecules," *Rev. Mod. Phys.* **70**, 1003-1025 (1998).
2. M. Shapiro and P. Brumer, *Principles of the Quantum Control of Molecular Processes*, (Wiley, New York, 2003).
3. D.J. Tanner and S. A. Rice, "Control of selectivity of chemical reaction via control of wavepacket evolution," *J. Chem. Phys.* **83**, 5013-5018 (1985).
4. M. Shapiro and P. Brumer, "Laser control of product quantum state populations in unimolecular reactions," *J. Chem. Phys.* **84**, 4103-4104 (1986).
5. R. S. Judson, H. Rabitz, "Teaching lasers to control molecules," *Phys. Rev. Lett.* **68**, 1500-1503 (1992).
6. A. M. Weiner, "Femtosecond pulse shaping using spatial light modulators," *Rev. Sci. Instrum.* **71**, 1929-1960 (2000).
7. T. C. Weinacht, J. Ahn, and P. H. Bucksbaum, "Controlling the shape of a quantum wavefunction," *Nature* **397**, 233-235 (1999).
8. H. Rabitz, R. de Vivie-Riedle, M. Motzkus, and K. Kompa, "Whither the future of controlling quantum phenomena?" *Science* **288**, 824-828 (2000).
9. N. Dudovich, B. Dayan, S. M. Gallagher Faeder, and Y. Silberberg, "Transform-limited pulses are not optimal for resonant multiphoton transitions," *Phys. Rev. Lett.* **86**, 47-50 (2001).
10. A. Monmayrant, B. Chatel, and B. Girard, "Quantum state measurement using coherent transients," *Phys. Rev. Lett.* **96**, 103002 (2006).
11. P. Nuernberger, G. Vogt, T. Brixner, and G. Gerber, "Femtosecond quantum control of molecular dynamics in the condensed phase," *Phys. Chem. Chem. Phys.* **9**, 2470-2497 (2007).
12. D. Meshulach and Y. Silberberg, "Coherent quantum control of two-photon transitions by a femtosecond laser pulse," *Nature* **396**, 239-242 (1998).

13. A. Assion, T. Baumert, M. Bergt, T. Brixner, B. Kiefer, V. Seyfried, M. Stehle, and G. Gerber, "Control of chemical reactions by feedback-optimized phase-shaped femtosecond laser pulses," *Science* **282**, 919-922 (1998).
14. R. J. Levis, G. M. Menkir, and H. Rabits, "Selective bond dissociation and rearrangement with optimally tailored, strong-field laser pulses," *Science* **292**, 709-713 (2001).
15. C. Trallero-Herrero, J.L. Cohen, and T. Weinacht, "Strong-field atomic phase matching," *Phys. Rev. Lett.* **96**, 063603 (2006).
16. H. Suchowski, A. Natan, B. D. Bruner, and Y. Silberberg, "Spatio-temporal coherent control of atomic systems: weak to strong field transition and breaking of symmetry in 2D maps," *J. Phys. B* **41**, 074008 (2008).
17. D. Meschulach, and Y. Silberberg, "Coherent quantum control of multiphoton transitions by shaped ultrashort optical pulses," *Phys. Rev. A* **60**, 1287-1292 (1999).
18. Z. Amitay, A. Gandman, L. Chuntunov, and L. Rybak, "Multichannel selective femtosecond coherent control based on symmetry properties," *Phys. Rev. Lett.* **100**, 193002 (2008).
19. N. Dudovich, T. Polack, A. Pe'er, and Y. Silberberg, "Simple route to strong-field coherent control," *Phys. Rev. Lett.* **94**, 083002 (2005).
20. P. Meystre and M. Sargent III, *Elements of Quantum Optics, 3rd ed.* (Springer-Verlag, Berlin, 1991).
21. A. Sieradzian, M. D. Havey, and M. S. Safronova, "Combined experimental and theoretical study of the  $6p^2P_j \rightarrow 8s^2S_{1/2}$  relative transition matrix elements in atomic Cs," *Phys. Rev. A* **69**, 022502 (2004).
22. P. Fendel, S. D. Bergeson, Th. Udem, and T. W. Hänsch, "Two-photon frequency comb spectroscopy of the 6s-8s transition in cesium," *Opt. Lett.* **32**, 701-703 (2007).
23. F. Verluise, V. Laude, Z. Cheng, Ch. Spielmann, and P. Tournois, "Amplitude and phase control of ultrashort pulses by use of an acousto-optic programmable dispersive filter: pulse compression and shaping," *Opt. Lett.* **25**, 575-577 (2000).

## 1. Introduction

Coherent control of a quantum system enables an involving nonlinear optical process to be optimized or steered through a desirable quantum path [1, 2]. This beautiful way of handling a quantum mechanical object was considered in early days to break chemical bonds, with a laser pulse pair [3], or with interference between continuous wave lasers [4]. Then, an optimal control theory with feedback algorithms was used to deal with complicated light-matter interactions [5]. The programming and maintaining the phase information contained in both the light and matter are central to the success of the control. For this, the ultrafast optical technique of programming spectral and temporal shapes of laser pulses, called ultrafast pulse shaping [6], has been developed. Lately the field of coherent control has been of significant interest in using shaped ultrafast pulses for the control of atomic and molecular dynamics [7, 8, 9, 10], even in condensed matter phase [11].

In a simple non-resonant two-photon absorption (i.e., no intermediate state to be considered), analytical studies of the dependence of the spectral phase of pulse shapes on the transition probability has been carried [12]. For a complex system, such an analytical approach is not easily applicable. Instead, in an adaptive approach, without requiring a priori knowledge of the system Hamiltonian a learning algorithm traces out a massive number of pulse shapes to search an optimal solution [5]. This adaptive approach has been useful to get nearly optimal pulse shapes for many light-matter interactions [13, 14, 15]. The adaptively found solutions sometimes fail to bring easy understanding of the underlying physics. Instead, an analytical control experiment with a few physical parameters in conjunction with an Hamiltonian analysis may better serve for this interest. Analytical controls of two-photon absorption have been carried out in the weak-field regime (i.e., when the field-induced level shift is negligible), and also in the strong-field regime [12, 16, 17, 18]. Most of these studies focus on Fourier domain shaping of laser pulses. However, in the strong-field interaction regime, a spectro-temporal domain study is necessary, because energy levels are time-dependent, shifted by the laser pulse. If the laser intensity is strong enough to induce a dynamic Stark shift more than laser bandwidth, the otherwise resonant (two-photon) condition for the absorption becomes no more satisfied, especially at the peak of the pulse. As in the weak interaction case [19], transform-limit is not an optimal shape in the strong-field interaction case, but with a different reason.

In this paper, we consider an analytical control of two-photon absorption process in the strong-field interaction regime. The performed experiment is a subclass of coherent controls, as the dynamic processes of the two-photon absorption are controlled by shaping the phase of laser pulses. However, to emphasize the difference from the adaptive controls [5], the term of analytical control is used instead. The experiment is carried out for the two-photon absorption of cesium by shaped ultrafast pulses from a programmable pulse-shaper. The fluorescence decay signal is investigated as a function of frequency chirp, detuning, and the pulse intensity in the vicinity of the weak-to-strong field crossover. The transition probability function is obtained as a solution of the time-dependent perturbation theory, and compared with the experimental results.

## 2. Control of Strong-Field Interaction

For a simple picture of the strong-field two-photon absorption, we consider control experiments with shaped laser pulses. Figure 1 depicts the schematics of experiments, with (a) a transform-limited pulse, (b) a positively-chirped pulse, (c) a negatively-chirped pulse, and (d) a red-detuned pulse. The corresponding energy diagrams of cesium are shifted temporally by the laser fields, as illustrated in the time and frequency plane. The spectrograms of the IR laser pulses are drawn in red and their second harmonic spectrograms are in blue.

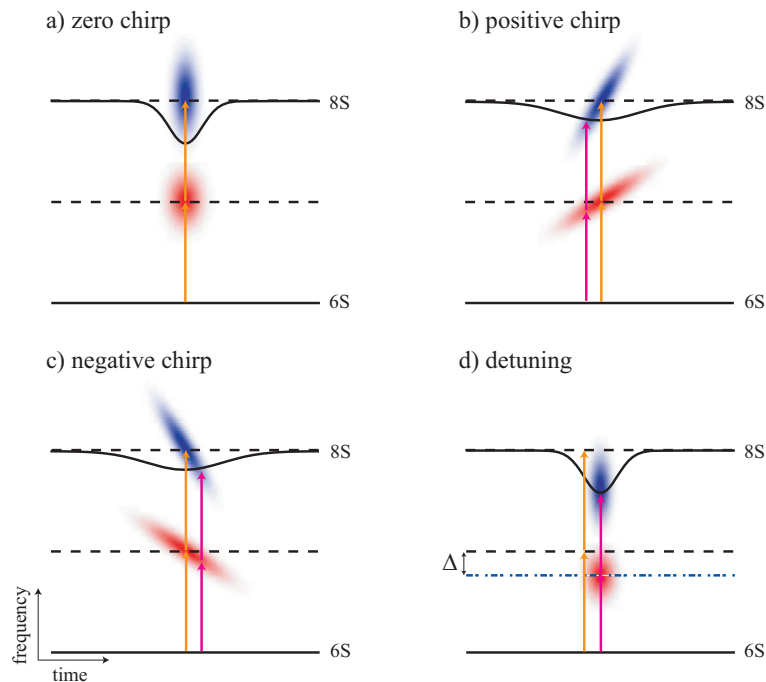


Fig. 1. Schematics of strong-field two-photon excitations of ground-state atomic cesium with shaped laser pulses. The spectrograms of the laser pulses and of their second harmonics are depicted in red and blue, respectively. The magenta arrows indicate the excitation paths for the strong interaction cases, while the yellow arrows do for the weak interaction cases.

Figure 1(a) shows the case when an un-shaped pulse strongly interacts with atoms. The dynamic Stark effect causes the two-photon excitation temporally off-resonant from the two-photon energy of the laser field. As a result, the most photons at the peak of the laser pulse do

not induce atomic excitation. The excitation is expected to happen not at the peak of the pulse, but more in both the head and tail of the temporal profile of the pulse. On the other hand, in Figs. 1(b) and 1(c), the laser pulses have positive and negative frequency chirps, but of the same pulse energies as in Fig. 1(a). These pulses shift the atomic energy levels less than Fig. 1(a) and, thereby, the atom-field resonant conditions for the two-photon absorption are better maintained. In particular, the Stark-shift energy levels can resonantly cross the spectro-temporal field densities in the second harmonic spectrograms (drawn in blue). We expect, therefore, to achieve stronger atomic excitations by both positively- and negatively-chirped pulses, than by a transform-limited pulse in Fig. 1(a). We note that the atomic excitation is expected to occur earlier in time than the peak of the pulse for the positively-chirped pulse as in Fig. 1(b), and later for the negatively-chirped pulse in Fig. 1(c). The Stark shift can be pre-compensated by a frequency-detuning of the laser pulse as illustrated in Fig. 1(d). Then, the atom-field resonant condition is satisfied at the peak of the pulse, and the pre-detuned pulse excites more than a pulse of zero detuning.

### 3. Theoretical Consideration

#### 3.1. Semiclassical Model Description

We consider a semiclassical Hamiltonian which describes a classical laser field interacting with quantum mechanical atoms. The  $6s$  state and  $8s$  state of cesium are used as the ground and excited state. The energy difference between the ground and excited state corresponds to 411 nm and the center wavelength of a laser pulse is 822 nm. The population of the  $6s$  state is excited to the  $8s$  state through a two-photon absorption process. The pulse involving two-photon transition has the center wavelength 822 nm and the bandwidth 30 nm. The energy between the intermediate state  $6p$  and the ground state corresponds to 852 nm and, therefore, the pulse can not approach the  $6p$  state sufficiently. Cesium atom can be considered as a two-level atom system. The Hamiltonian of a strong-field two-level atom system can be written as [20]:

$$\mathbf{H}(\mathbf{t}) = \begin{pmatrix} \omega_g^{(S)}(t) & \chi^*(t)e^{-i[\delta t - \phi(t)]} \\ \chi(t)e^{i[\delta t - \phi(t)]} & \omega_e^{(S)}(t) \end{pmatrix}, \quad (1)$$

where the two-photon detuning is given as  $\delta = 2\Omega - \omega_{eg}$  and  $\phi(t)$  is the temporal phase of the pulse to be applied to the atom system.  $\omega_g^{(S)}(t)$  and  $\omega_e^{(S)}(t)$  are the Stark shifted angular frequencies of the ground and excited states, each states is coupled with the far-detuned intermediate states:

$$\omega_{e,g}^{(S)}(t) = -\sum_m \frac{\mu_{\{e,g\}m}^2}{\hbar^2} \frac{I g(t)}{c\epsilon_0} \frac{\omega_{m\{e,g\}}}{\omega_{m\{e,g\}}^2 - \Omega^2}, \quad (2)$$

where the two-photon Rabi frequency  $\chi(t)$  represents two-photon coupling of the excited state and the ground state:

$$\chi(t) = -\sum_m \frac{\mu_{em}\mu_{mg}}{2\hbar^2} \frac{I g(t)}{c\epsilon_0} \frac{1}{\omega_{mg} - \Omega}. \quad (3)$$

Here,  $\mu_{em}(\mu_{mg})$  is transition dipole moments between the excited(ground) and intermediate states.  $\omega_{m\{e,g\}}$  is defined as  $\omega_{m\{e,g\}} = \omega_m - \omega_{\{e,g\}}$  where  $\omega_m$  and  $\omega_{\{e,g\}}$  are the angular frequencies of the intermediate and excited(or ground) states.  $I$  is the peak intensity and  $\epsilon_0$  is the permittivity of free space.  $g(t)$  is the temporal intensity profile given as  $g(t) = \exp(-t^2/\tau^2)$ . The excited population was measured via fluorescence from the  $7p$  state.

To estimate the final population of the excited state, an atom-field phase  $\alpha(t)$  can be used:

$$\alpha(t) = \int_{-\infty}^t \Delta(t') dt' - \delta t + \phi(t), \quad (4)$$

where  $\Delta(t)$  is defined as  $\Delta(t) = \omega_e^{(s)}(t) - \omega_g^{(s)}(t)$ . Generally, a strong-field phase matching condition is maximizing the integral [15]:

$$\left| \int_{-\infty}^{\infty} \chi(t) \exp[i\alpha(t)] dt \right|^2 \quad (5)$$

for the fixed pulse area, such that  $\int_{-\infty}^{\infty} \chi(t) dt = \pi/2$ . If the atom-field phase is perfectly matched, the integral is maximum. It is not proportional to the excited population exactly but shows the predisposition that the excited population is getting larger when the value of the integral is increasing. We calculate the quantity of the phase matching condition to estimate the excited population. The strong-field phase matching makes it possible to estimate the excited population by an analytic form. The phase term  $\alpha(t)$  increases rapidly with time. We expand  $\alpha(t)$  using  $t/\tau$  parameter.

$$\alpha(t) \simeq \frac{\sqrt{\pi}}{2} \Delta \tau \left[ 1 + \left(\frac{t}{\tau}\right) - \frac{1}{3} \left(\frac{t}{\tau}\right)^3 + \dots \right] - \delta t + \beta t^2, \quad (6)$$

where the temporal phase  $\phi(t) = \beta t^2$  for a linear chirp pulse is considered. The strongest field around time-zero contributes to the excited population dominantly. In  $|t| < \tau$  region, the first term of  $\alpha(t)$  is approximated to a linear function. And  $\chi(t)$  is decreasing exponentially in  $|t| > \tau$ . Thus the contribution of higher order terms of  $t/\tau$  is relatively small. Higher order terms up to the third order could be neglected. After integration, we obtain the following expression of the excited population:

$$P_e \propto \chi_0^2 \frac{\pi \tau^2}{\sqrt{1 + \beta^2 \tau^4}} \exp \left[ -\frac{(\delta - \Delta \sqrt{\pi}/2)^2 \tau^2}{2(1 + \beta^2 \tau^4)} \right] \quad (7)$$

In the case of zero detuning and weak field,  $\delta$  and  $\Delta$  go to zero. Thus the excited population is described as:

$$P_e \propto \frac{1}{\sqrt{1 + \beta^2 \tau^4}} \quad (8)$$

It has a single symmetrical peak at zero chirp rate and the perturbation approach also gives the same form of the excited population. In strong field and zero detuning, only  $\delta$  goes to zero. The excited population is given as:

$$P_e \propto \frac{1}{\sqrt{1 + \beta^2 \tau^4}} \exp \left[ -\frac{\pi \Delta^2 \tau^2}{8(1 + \beta^2 \tau^4)} \right] \quad (9)$$

It has two peaks at the certain negative and positive chirp rate. It shows the minimum at zero chirp rate.

### 3.2. Dynamic Stark Shift in Cesium

We calculate the dynamic Stark shift of the  $6s$  and  $8s$  state of cesium. The ground state  $6s$  and excited state  $8s$  couple to the intermediate states with angular momentum quantum number  $l > 0$ , which is far from the resonance [21]. We neglect couplings to the intermediate states with  $l > 1$  because the ground and excited state have an angular momentum of  $l = 0$ . By the angular momentum selection rule,  $\Delta l = -1, 0, 1$ , couplings to the p states are dominant. And the transition dipole moment has a significant value when total angular momentum selection rule  $\Delta j = -1, 0, 1$  are satisfied. The s states are able to couple to not only the  $p_{1/2}$  states but also  $p_{3/2}$ . Because the  $6p_{3/2}$  state is not enough far from the resonance, it does not couple to the  $6s$  state. The sum of shift in the transition from  $6s_{1/2}$  determines the total dynamic Stark shift. The  $6s$  ground state and the  $8s$  excited state shift 20.87 THz and 14.15 THz for the pulse intensity of  $1 \times 10^{11}$  W/cm<sup>2</sup>. Both are up-shifted but the shift of the  $6s$  state is larger than the  $8s$  state. Therefore the energy level difference is smaller [22] by -6.72THz.

#### 4. Experimental Setup

For the experiment, a Ti:sapphire laser amplifier system is used to produce 150-fs-short pulses with a pulse energy of 100  $\mu\text{J}$  at a repetition rate of 1 kHz. The wavelength of the laser is centered at about 822 nm. The laser pulse passes through an actively controlled acousto-optic programmable dispersive filter (DAZZLER) [23], which controls the phase and amplitude of an ultrafast pulse. It overcomes the two limitations of a spatial light modulator: free of coupling of the spatial and temporal aberrations of the laser beam and providing for large dispersion compensation ranges. The pulse shaper writes a polynomial function of the power spectrum of the pulse,  $A(\omega)e^{i\Phi(\omega)}$ . The spectral phase  $A(\omega)$  is programmed as

$$\Phi(\omega) = a_1(\omega - \Omega) + \frac{a_2}{2}(\omega - \Omega)^2 + \frac{a_3}{6}(\omega - \Omega)^3 + \frac{a_4}{24}(\omega - \Omega)^4 + \dots, \quad (10)$$

where  $a_1$  is the delay parameter.  $a_2$ ,  $a_3$ , and  $a_4$  are the second, the third, and the fourth order chirp parameters. In the experiment, the second-order chirp  $a_2$  is varied from  $-4 \times 10^4$  to  $4 \times 10^4$   $\text{fs}^2$ . The apertured pulse is focused on a cesium vapor cell by a lens of  $f = 125$  mm. A lens of shorter focal length induces a short Rayleigh range and it cause a longitudinal intensity averaging effect. The focused spot on the vapor cell is imaged by a telescope into the photomultiplier (PMT, Hamamatsu R1527P). Additionally, a bandpass filter for 460 nm is inserted before the PMT to block the undesirable fluorescence and scattered IR. The signal intensity of the PMT is kept in the well-calibrated detection range so that the fluorescence signal from  $7p$  is linearly measured. The excited  $8s$  population is below the saturation limit and is linearly mapped with the fluorescence signal. The experimental setup is shown in Fig. 2.

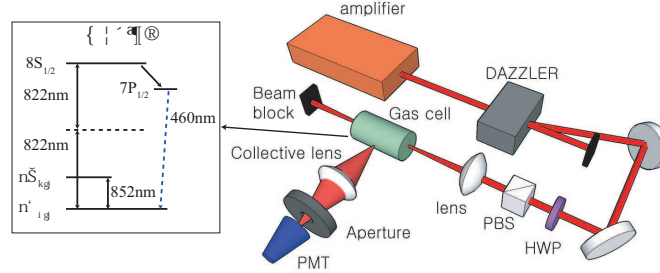


Fig. 2. Schematic setup of a shaped-pulse two-photon absorption experiment in atomic cesium. A half-wave plate (HWP) and a polarization beam splitter (PBS) are used to vary the peak intensity for the range of  $0 - 2 \times 10^{11}$   $\text{W}/\text{cm}^2$ . The inset shows the energy levels of atomic cesium.

#### 5. Results and Discussions

In our experiment, we have changed the chirp rate  $a_2$ , not  $\beta$ . As  $\tau$ ,  $\beta$ ,  $\Delta$ , and  $\chi_0$  are functions of  $a_2$ , a linear chirp rate in frequency domain, these parameters satisfy the following relations from the Fourier transform:

$$\beta\tau^2 = 2a_2/\tau_0^2, \quad (11)$$

$$\Delta\tau = \Delta_0\tau_0, \quad (12)$$

$$\chi_0\tau = \chi_0^{(0)}\tau_0, \quad (13)$$

where  $\tau_0$  is the pulse duration at zero chirp rate.  $\Delta_0$  and  $\chi_0^{(0)}$  are the amplitude of the dynamic Stark shift and the amplitude of the two photon coupling at time-zero with an unshaped pulse.

After substitution the Eq. (11)-(13) to the Eq. (7), the formula of the excited population is obtained:

$$P_e \propto \frac{1}{\sqrt{1+4a_2^2/\tau_0^4}} \exp \left[ -\frac{1}{2} \left( \delta\tau_0 - \frac{\sqrt{\pi}\Delta_0\tau_0}{2\sqrt{1+4a_2^2/\tau_0^4}} \right)^2 \right]. \quad (14)$$

### 5.1. Intensity Dependence

To observe the effect of the dynamic Stark shift which is dependent on the pulse intensity, we measure the 7p-6s fluorescence as a function of chirp rate  $a_2$  and pulse peak intensity. However, the pulse peak intensity is also a function of  $a_2$ , we use instead unshaped-pulse peak intensity, or the intensity of the corresponding transform-limited (TL) pulse. So, we denote  $I_0$  for the TL peak intensity of a given shaped pulse, where  $I_0 = I\tau/\tau_0$  and  $\tau = \tau_0\sqrt{1+(2a_2/\tau_0)^2}$ . The experimental data and the fitted lines are given in Fig. 3. From the Eq. (7), we obtain the fitting formula of the fluorescence as a function of a chirp rate  $a_2$  which can be controlled in our experiment:

$$P_e \propto \frac{1}{\sqrt{1+4a_2^2/\tau_0^4}} \exp \left[ -\frac{\pi\eta^2 I_0^2 \tau_0^2}{8(1+4a_2^2/\tau_0^4)} \right], \quad (15)$$

where  $\eta$  is a proportional coefficient. The experimental data was fitted by Eq. (15), the pulse duration  $\tau_0$  is fixed at 88 fs. Eq. (15) contains two terms; the first term has a single peak at zero chirp rate which is caused by the effect of fixed levels. The second term has the minimum at zero chirp rate due to the dynamic Stark shift. The two terms compete with each other; In weak field, the first term dominates the second term and the single peak shape is presented as shown in Fig. 3(b). While the pulse intensity is growing, the second term is dominant and a dip at zero chirp becomes deeper and wider. Therefore the double peak shape is arising as shown in Fig. 3(c).

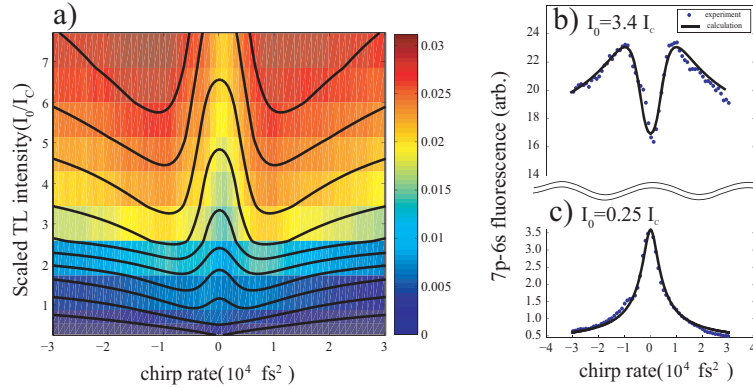


Fig. 3. (a) Measured 7p-6s fluorescence signal induced by two-photon absorption in atomic cesium is plotted in color (red is the biggest) as a function of linear chirp rate  $a_2$  and scaled TL peak intensity  $I_0/I_c$ . The equi-signal levels are traced by contour lines which are reconstructed by a model calculation with best fit parameters. The typical behaviors of the signals are shown in the strong- and weak-field regimes in (b) and (c), respectively.

To estimate the onset TL intensity between the weak and strong field, we approximate

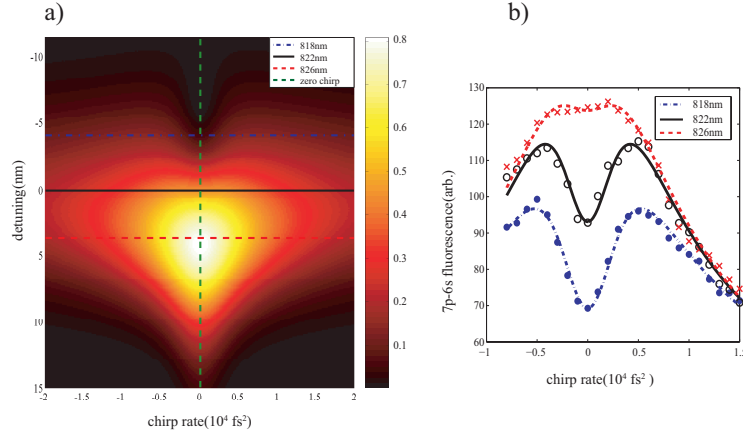


Fig. 4. (a) Calculated  $7p-6s$  fluorescence signals of atomic cesium in color (white is the biggest), plotted as a function of linear chirp rate and detuning. The TL intensity is  $I_0 = 1.43I_c$ . (b) Measured  $7p-6s$  fluorescence as a function of chirp rate

Eq. (15) around zero chirp:

$$P_e \propto \left[ 1 + \frac{1}{8} \pi \eta^2 \tau_0^2 (I_0^2 - I_c^2) \left( \frac{2a_2}{\tau_0^2} \right)^2 \right] \exp \left( -\frac{\pi \eta^2 \tau_0^2 I_0^2}{8} \right). \quad (16)$$

It is a quadratic function of  $a_2$ . The sign of  $I_0^2 - I_c^2$  determines whether a function is upward or downward opened parabola and the onset intensity is  $I_c = 2/\sqrt{\pi} \eta \tau_0$ . If the pulse peak intensity is sufficiently high (low), the fluorescence function is upward (downward) opened parabola around zero chirp rate and has a single peak (double peak). In our experiments,  $\eta$  is given as  $-50.4 \text{ Trad/s}$  at the  $I_0 = 1 \times 10^{11} \text{ W/cm}^2$  with a 150 fs laser pulse. Thus the onset peak intensity is calculated as  $I_c = 0.25 \times 10^{11} \text{ W/cm}^2$  in our experiments. Over the onset intensity, symmetrical double peak shape becomes clear as shown in Fig. 3(a). It means that the use of the certain negatively or positively chirped pulse is able to maximize the fluorescence. As a peak intensity is growing with the fixed pulse duration, the level energy difference is varying rapidly. Thus a larger chirped pulse can make the resonance region, maximizes the fluorescence. As shown in Fig. 3, an interval between two peaks is lengthened due to the stronger dynamic Stark shift.

### 5.2. Center Frequency Detuning

Generally, the fluorescence has a single peak in weak field and double peaks in strong field. But, a single peak line shape is recovered at the certain detuning, even in strong field. The strongest field of the pulse at time zero, which mainly influences the excited population, is able to keep the resonance on the two photon transition when the center frequency of the pulse is shifted. In this case, a linearly-chirped pulse (frequency-swept pulse) breaks the resonance and the excited population is reduced. From the Eq. (14), the  $7p-6s$  fluorescence can be calculated as a function of chirp rate  $a_2$ , detuning  $\delta$ , and TL intensity  $I_0$ . In the case that  $I_0$  is fixed at  $1.43I_c$ , the calculated fluorescence is plotted in Fig. 4(a) and the corresponding experimental data is given in Fig. 4(b). The equi-signal line in Fig. 4(a) is written as:

$$C = \frac{1}{2} X^2 - \frac{\sqrt{\pi}}{4} \eta I_0 \tau_0^2 X^2 Y + \frac{\tau_0^2}{2} Y^2, \quad (17)$$

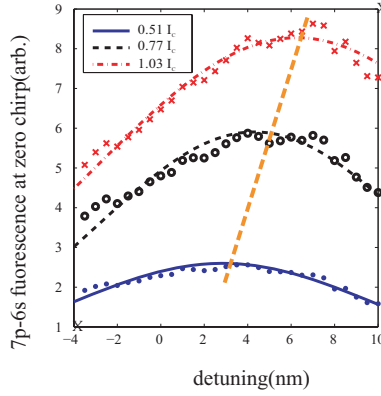


Fig. 5. Measured  $7p$ - $6s$  fluorescence signals in symbols as a function of detuning at various fixed peak intensities, compared with numerical fits in lines using Eq. (18).

where  $X = 2a_2/\tau_0^2$  and  $Y = \sqrt{\pi}\eta I_0/2 - \delta$ .  $C$  is a constant related to the magnitude of the fluorescence.  $X$  and  $Y$  are the scaled chirp rate and detuning. Eq. (17) is a formula of a looped curve (a heart shape). In weak field, the pulse intensity goes to 0 and the curve becomes the circle centered at the origin. If the pulse intensity is enough to induce the sufficiently large dynamic Stark shift, the circle is distorted and becomes a shape of an inverted triangle centered at the detuning of  $\delta_p = \sqrt{\pi}\eta I_0/2$ . Around the detuning of  $\delta_p$ , the single peak is recovered and, from the Eq. (14), the maximum fluorescence is obtained at zero chirp rate. Because the difference of the dynamic Stark shifts is negative in cesium, the detuning for resonance is also negative. As a result, the fluorescence maximum is obtained at the condition of (detuning, chirp rate) =  $(\delta_p, 0)$  at a given  $I_0$ , as expected in Fig. 4(a).

In our experimental condition, the detuning  $\delta_p$  is about 5.6 nm at the TL intensity  $I_0 = 1.43I_c$ . Figure 5 shows the  $7p$ - $6s$  fluorescence measured as a function of the detuning along the green dashed line in Fig. 4(a). The chirp rate is fixed at 0. The formula of the  $7p$ - $6s$  fluorescence for the fixed chirp rate is obtained from Eq. (14) as

$$P_e \propto \exp(-(\delta - \Delta_0\sqrt{\pi}/2)^2\tau_0^2/2). \quad (18)$$

The detunings are 2.8 nm, 4.3 nm, and 6.2 nm for  $I_0 = 0.51I_c$ ,  $0.77I_c$ , and  $1.03I_c$ , respectively. In Fig. 5, the detuning for the compensation of the dynamic Stark shift is found proportional to  $I_0$ , showing good agreement with Eq. (18).

## 6. Conclusion

We have experimentally demonstrated that transform-limited pulse shapes are not optimal for the strong-field two-photon transitions, even in the case when intermediate states are off-resonant as in atomic cesium. It turns out that a shaped pulse with a non-zero chirp rate, either a positive or negative, is more efficient, in the strong-field interaction regime, than an unshaped pulse is. A semiclassical model calculation shows excellent agreements with the investigated phenomenological relationship among the laser detuning, the chirp-rate, and the temporal intensity shape of the laser pulse obtained for the optimal two-photon transition in atomic cesium.

## **Acknowledgments**

We thank C. H. Nam for the Dazzler pulse shaper and also for many discussions. This work was supported by MOHERD Grant KRF-2005-205-C00024 and IT R&D program of MKE/IITA 2008-F-021-01.